Biomedicine & Pharmacotherapy 86 (2017) 628–636

Available online at
ScienceDirect
www.sciencedirect.com

Elsevier Masson France
EM|consulte
www.em-consulte.com/en

Original article

Construction and comparison of different nanocarriers for co-delivery of cisplatin and curcumin: A synergistic combination nanotherapy for cervical cancer

Changming Li, Xiangcheng Ge, Liguo Wang*

Department of Pharmacy, Linyi People's Hospital, Linyi, Shandong, PR China

ARTICLE INFO

Article history:
Received 1 September 2016
Received in revised form 28 November 2016
Accepted 8 December 2016

Keywords:
Synergistic combination nanotherapy
Co-delivery
Lipid-polymer hybrid nanoparticles
Polymeric nanoparticles
Cisplatin
Curcumin

ABSTRACT

Purpose: Co-delivery of two or more drugs into the same cancer cells or tissues in the same nanocarriers provides a new paradigm in cancer treatment. In this study, two kinds of nanocarriers: lipid-polymer hybrid nanoparticles (LPNs) and polymeric nanoparticles (PNPs) were constructed and compared for co-delivery of cisplatin (DDP) and curcumin (CUR).
Methods: DDP and CUR loaded LPNs (D/C/LPNs) and PNPs (D/C/PNPs) were prepared. Two kinds of nanocarriers were characterized in terms of particle size, zeta potential, drug encapsulation efficiency (EE), and drug release. Their *in vitro* cytotoxicity and *in vivo* anti-tumor efficacy was studied on human cervix adenocarcinoma cell line (HeLa cells) and mice bearing cervical cancer model.
Results: Compared with D/C/PNPs, D/C/LPNs showed significantly higher cytotoxicity *in vitro*. D/C/LPNs also displayed the best antitumor activity than other formulations tested *in vivo*.
Conclusions: The results demonstrated that LPNs could improve the anticancer efficacy of drugs to higher levels than PNPs and free drugs, thus could serve as an effective drug system for targeted and synergistic co-delivery nanomedicine for cervical cancer chemotherapy.

1. Introduction

Cervical cancer, with an incidence of 528,000 worldwide in 2012, is one of the most common cause of cancer-related deaths in females, with 85% of cases occurring in developing countries where cervical cancer is a leading cause of cancer death in females [1–4]. Based on the latest version of NCCN guidelines for cervical cancer (Version 1. 2015), cisplatin (DDP) alone or in combination with paclitaxel has been recommended as the first-line single-agent therapy or the first-line combination therapy for advanced stage, recurrent or metastatic cervical cancer [5,6] However, the dose limiting toxicities (nephrotoxicity and hepatotoxicity) and drug resistance associated with DDP has presented a serious concern in clinic [7–10]. Combination chemotherapy and nanocarrier-based delivery of DDP to the tumor sites are the most two areas of intense researches to solve the aforementioned problems [11–13].

Curcumin (CUR) is the natural compound extracted from the rhizome of turmeric (*Curcuma longa*) that allows suppression, retardation and inversion of carcinogenesis [14]. The molecular mechanism of CUR induced cytotoxicity in cervical cancer cells possess multiple targets including inhibition of telomerase; inhibition of cyclin D1 and CDK4 via acetylation and upregulation of p53, leading to cell cycle arrest at G1/S phase; induction of endoplasmic reticulum stress-mediated apoptosis, etc [15–17]. Furthermore, CUR can reverse the multi-drug resistance (MDR) of cancer cells [18]. DDP resistance in SiHaR due to over-expression of MRP1 and Pgp1 was overcome by CUR [19]; and the nephrotoxicity of DDP can be reduced by CUR, thereby enhancing the therapeutic window of DDP [10]. However, because of the hydrophobic properties of DDP and CUR, it is necessary to engineer ideal nanocarriers to co-delivery DDP and CUR to the tumor tissues at the same time.

Nanocarrier-based delivery of anticancer drugs has received much attention in recent years because of its potential for

* Corresponding author at: Department of Pharmacy, Linyi People's Hospital, No. 27 Jiefangludongduan, Linyi, 276003, Shandong Province, PR China.
E-mail address: wlglyph@163.com (L. Wang).

http://dx.doi.org/10.1016/j.biopha.2016.12.042
0753-3322/

improving drug efficacy, reducing unwanted side effects and circumventing cellular accumulation mediated drug resistance. Of all the common nanoparticulate systems, liposomes and biodegradable polymeric nanoparticles (PNPs) have emerged as the two dominant classes of drug nanocarriers, as evidenced by increasing numbers of approved drug products, clinical trials, and research reports [20,21]. Lipid-polymer hybrid nanoparticles (LPNs), combing the mechanical advantages of biodegradable PNPs and biomimetic advantages of liposomes, are core-shell nanoparticles structures comprising polymer cores and lipid/lipid-PEG shells [22,23]. The hybrid architecture of LPNs can provide advantages such as entrapment of multiple therapeutic agents, high drug loading, controllable particle size, good serum stability, etc. Therefore, lipid-polymer hybrid nanoparticles (LPNs) were constructed for co-delivery of cisplatin (DDP) and curcumin (CUR), and compared with PNPs.

In the present study, DDP and CUR loaded LPNs (D/C/LPNs) and PNPs (D/C/PNPs) were prepared. The physicochemical properties of the two kinds of nanocarriers were characterized including particle size, zeta potential, drug encapsulation efficiency (EE), and drug release. *In vitro* cytotoxicity and *in vivo* anti-tumor efficacies were studied on human cervix adenocarcinoma cell line (HeLa cells) and mice bearing cervical cancer model. LNPs were anticipated to serve as an effective delivery platform for targeted and synergistic co-delivery DDP and CUR for cervical cancer chemotherapy.

2. Materials and methods

2.1. Materials

Cisplatin (DDP) was provided by Shandong Boyuan Pharmaceutical Co., Ltd (Ji'nan, China). Curcumin (CUR) was obtained from Ji'nan Guoshiweiye Chemical Co., Ltd (Ji'nan, China). Poly (lactic-co-glycolic acid) (PLGA, molar ratio of D, L-lactic to glycolic acid, 50: 50) was purchased from Ji'nan Daigang Biotechnology Co. Ltd. HeLa cells and human umbilical vein endothelial cells (HUVEC) were obtained from the American type culture collection (Manassas, VA). PEG-DSPE was purchased from Xi'an Ruixi Biological Technology Co., Ltd (Xi'an, China). Cholesterol, 3-(4,5-dimehyl-2-thiazolyl)-2,5-diphenyl-2H-tetrazolium bromide (MTT), and Pluronic F68 were purchased from Sigma-Aldrich Co., Ltd (St Louis, MO). All other chemicals were of analytical grade or higher.

BALB/c nude mice (18–22 g weight) were purchased from the Beijing Fuzhong Technology Development Co., Ltd (Beijing, China). All animal experiments complied with the Animal Management Rules of the Ministry of Health of the People's Republic of China.

2.2. Preparation of LPNs and PNPs

D/C/LPNs were prepared by the nanoprecipitation technology [24]. In detail, PLGA (100 mg), DDP (20 mg) and

Table 1
Characterization of LPNs and PNPs.

Characteristics	D/C/LPNs	D/LPNs	C/LPNs	D/C/PNPs	LPNs	PNPs
Particle size (nm)	163.4 ± 7.52	141.5 ± 5.13	151.4 ± 8.23	118.5 ± 4.62	110.3 ± 3.19	91.6 ± 2.94
PDI	0.16 ± 0.05	0.14 ± 0.03	0.19 ± 0.06	0.15 ± 0.04	0.12 ± 0.03	0.11 ± 0.02
Zeta potential (mV)	−19.6 ± 2.62	−11.9 ± 1.81	−25.8 ± 3.78	−13.7 ± 1.36	−21.3 ± 2.31	−15.6 ± 2.08
EE of DDP (%)	88.7 ± 6.81	89.5 ± 5.32	N/A	83.3 ± 3.89	N/A	N/A
EE of CUR (%)	85.2 ± 4.14	N/A	84.6 ± 3.72	81.5 ± 6.79	N/A	N/A
DL of DDP (%)	1.91 ± 0.31	1.96 ± 0.42	N/A	2.02 ± 0.56	N/A	N/A
DL of CUR (%)	9.1 ± 1.62	N/A	8.9 ± 1.34	8.7 ± 1.49	N/A	N/A

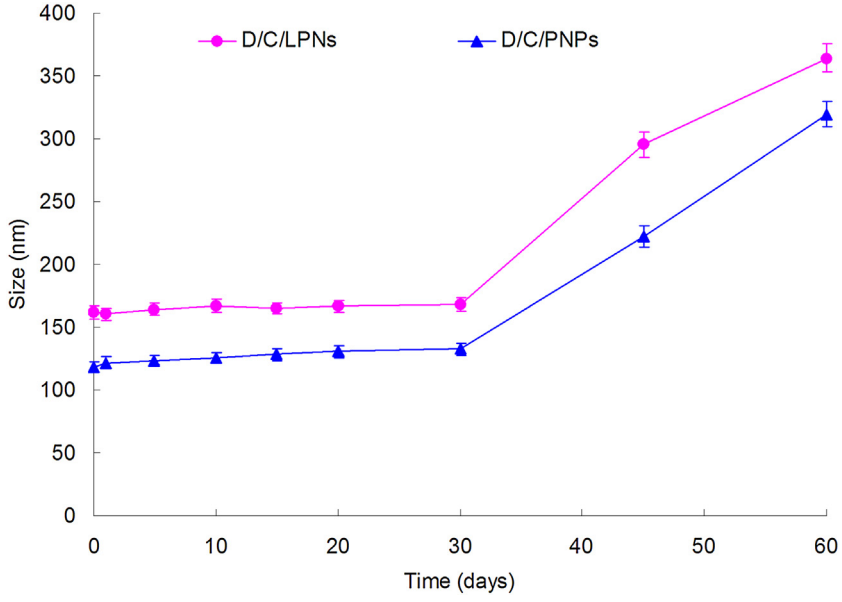

Fig. 1. The average diameter of D/C/LPNs and D/C/PNPs during 60 days.

CUR (40 mg) were dissolved in dimethylsulfoxide (3 mL). Lecithin, and DSPE-PEG (4:1, molar ratio) with a weight ratio of 12% to the PLGA were dissolved in 4% ethanol and heated to 60 °C under stirring. PLGA solution was simultaneously and separately added dropwise into the lipid solution under gentle stirring. Then the solution was vortexed for 5 min. The mixture was stirred at 600 rpm for 1 h at room temperature. The organic solvent was removed by dialyzed method: dialyzed (MWCO: 12 000–14000, Spectrum Laboratories Inc., Laguna Hills, CA) against Milli-Q water for 12 h. Finally, D/C/LPNs were obtained by washing the mixture several times by centrifugation for 20 min at 1500 rpm at 4 °C for each time. DDP loaded LPNs (D/LPNs) and CUR loaded LPNs (C/LPNs) were prepared using the same method in the presence of one single drug. Blank LPNs without drug were also prepared as control.

DDP and CUR loaded PNPs (D/C/PNPs) were prepared as follows [25,26]: PLGA (100 mg), DDP (20 mg) and CUR (40 mg) were dissolved in dimethylsulfoxide (3 mL). The organic phase was added drop-wise into a desired aqueous stabilizer of 1% Pluronic F68 (w/v) being stirred at 600 rpm at room temperature. The organic solvent was removed by dialyzed method: dialyzed against Milli-Q water for 12 h. Finally, D/C/PNPs were obtained by washing the mixture several times. Blank PNPs without drug were also prepared as control.

2.3. Characterization of LPNs and PNPs

The size (diameter, nm), polydispersity index (PDI), and surface charge (zeta potential, mV) of LPNs and PNPs was determined by Malvern Zetasizer Nano ZS (Malvern Instrument Ltd., Worcestershire, UK).

The DDP encapsulation efficiency (EE) and loading capacity (DL) of LPNs and PNPs were measured by using the HITACHI P-4010 inductively coupled plasma mass spectrometry (ICP-MS) (Hitachi Ltd, Kyoto, Japan) [13]. Briefly, 5 mL LPNs or PNPs were centrifuged (10000 rpm, 4 °C, 20 min) separately, and the supernatants were then determined using the ICP-MS. The CUR EE of LPNs and PNPs was measured by absorbance using UV–vis spectroscopy at 430 nm.

The EE and DL was calculated as follows:

EE (%) = (The weight of total drug − the weight of free drug)/the weight of total drug × 100.

DL (%) = (The weight of total drug − the weight of free drug)/the weight of drug and NPs × 100.

2.4. Stability of LPNs and PNPs

The stability of D/C/LPNs and D/C/PNPs over 60 days was investigated by monitored the size variation [27]. Changes in size distribution and were used to evaluate stability.

2.5. Drug release from LPNs and PNPs

To measure the release profile of DDP or CUR from LPNs and PNPs, the formulations were incubated in phosphate buffers (PBS, pH 7.4), which were constant shaking at 37 °C [28]. At predetermined time points, the media was taken out and replaced with fresh media. The DDP or CUR content was determined by the method mention in the above section.

2.6. In vitro cytotoxicity assays of LPNs and PNPs

The cytotoxicity of LPNs and PNPs was tested in HeLa cells and HUVEC using the MTT assay [29]. Briefly, cells were seeded in a 96-well plate at a density of 3000 cells/well and allowed to adhere for 24 h prior to the assay. Then, cells were treated with D/C/LPNs, D/LPNs, C/LPNs, D/C/PNPs, DDP and CUR mixed solution (D/C solution), DDP solution, CUR solution, LPNs, PNPs, and 0.9% saline (as the control group) at various concentrations for 48 h at 37 °C and 5% CO_2 atmosphere, respectively. Culture medium was used as the blank group. Then, MTT dye, at a concentration of 5 mg/ml was added to each well and cells were incubated for 4 h at 37 °C. 200 μL of DMSO was added to each well to dissolve the MTT formazan crystals. The optical density (OD) of formazan product was measured using a microplate reader (Model 680, BIO-RAD, USA) at 570 nm. The relative cell viability (CV) was calculated as follows: CV(%) = (OD of the sample group − OD of the blank group)/(OD of the control group − OD of the blank group) × 100. The DDP and CUR concentration causing 50% of cells inhibition (IC_{50}) was calculated.

2.7. Synergistic effect of drugs loaded in LPNs and PNPs

Synergistic effects in terms of tumor cell proliferation inhibition

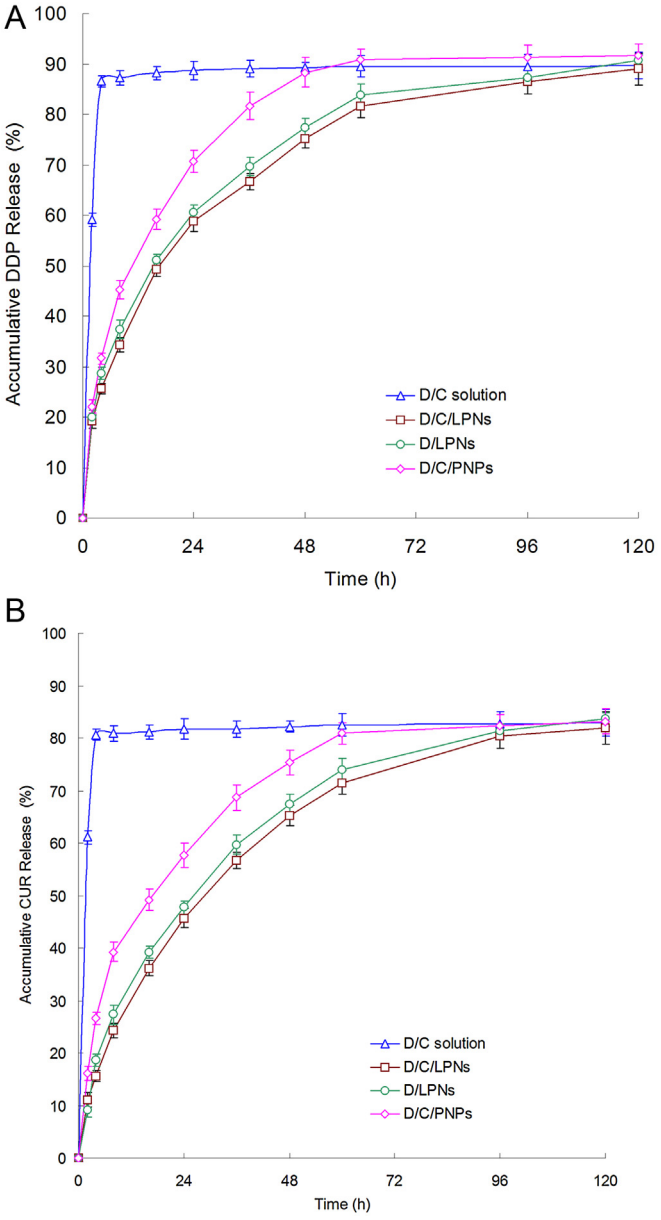

Fig. 2. Release of DDP (A) and CUR (B) from LPNs, PNPs and solutions.

ability of drugs loaded LPNs and PNPs were evaluated against HeLa cells after 48 h of incubation. The inhibitory concentration (ICx) values were determined using Origin 8.0 (OriginLab, Northampton, MA). The Combination Index (CI) was measured according to the Chou and Talalay's method [30]. The equation $CI_x = (D)_1/(D_x)_1 + (D)_2/(D_x)_2$ was used to distinguish synergistic, additive, or antagonistic cytotoxic effects. In which $(D_x)_1$ and $(D_x)_2$ represent the ICx value of DDP and CUR alone, respectively. $(D)_1$ and $(D)_2$ represent the concentration of DDP and CUR in the combination system at the ICx value. $CI > 1$ represents antagonism, $CI = 1$ represents additive and $CI < 1$ represents synergism. In this study, IC_{50} (inhibitory concentration to produce 50% cell death) was applied.

2.8. In vivo *organ distribution study*

The cervical cancer bearing BALB/c nude mice model was used to investigate the *in vivo* organ distribution of LPNs [31]. To prepare the cervical cancer bearing animal models, mice were subcutaneously injected at the right armpit with 0.1 mL of cell suspension containing 10^5 of HeLa cells suspended in PBS for 24 h. When the volume of the tumor reached about 100 mm^3, the cervical cancer bearing mice were divided into three groups. The first group served as control, which was maintained on the same regular diet throughout study period. The other two groups was administered 1 mL of D/C/LPNs, or D/C/PNPs through the tail vein, separately. Three animals from each group were killed by deep ether anesthesia at 1, 2, 4, 8, 24 and 48 h after drug administration. The tumor, heart, liver, spleen, lung and kidney of mice were isolated. The organs were cut into small pieces and homogenized by Micro Tissue Homogenizer at 4 °C along with a small amount of HPLC grade water. One milliliter of methanol was added to tissue homogenate and kept for 30 min. The contents were centrifuged at 5000 rpm for 10 min and the supernatant liquid was separated. After appropriate dilution of supernatants, the drug content was determined by HPLC method. The DDP and CUR drug at different time intervals was calculated by the method as described in the "Determination of drug loading and entrapment efficiency" section.

2.9. In vivo *anti-tumor assays of LPNs and PNPs*

The cervical cancer bearing BALB/c nude mice model was used to investigate the *in vivo* antitumor efficacy of LPNs [31]. When the volume of the tumor reached about 100 mm^3, the cervical cancer bearing mice were divided into 9 groups (8 mice per group): The D/C/LPNs, D/LPNs, C/LPNs, D/C/PNPs, D/C solution, DDP solution, CUR solution, LPNs, PNPs, and 0.9% saline were prepared and injected intravenously into the mice via the tail vein. The amounts of drugs used for each group in the above formulations were: 1 mg DDP per kg of mice and 5 mg CUR per kg of mice. The first day of administration was designated day 0, and administration was then

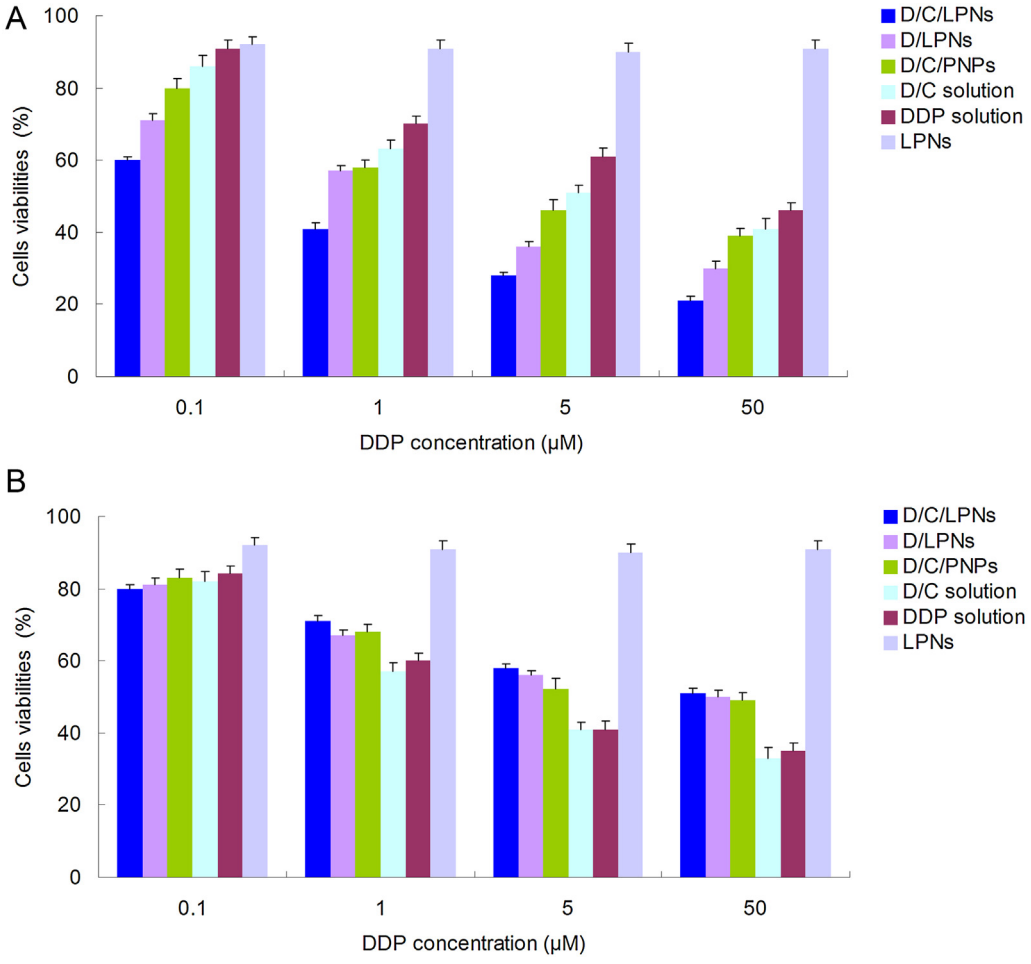

Fig. 3. *In vitro* cytotoxicity of LPNs and PNPs on HeLa cells (A) and HUVEC (B).

Table 2
IC_{50} values of LPNs and PNPs.

Formulations	D/C/LPNs	D/LPNs	C/LPNs	D/C/PNPs	D/C solution	DDP solution	CUR solution
DDP IC_{50} (μM)	0.8 ± 0.12	2.3 ± 0.34	N/A	4.3 ± 0.41	5.2 ± 0.63	7.1 ± 0.95	N/A
CUR IC_{50} (μM)	1.6 ± 0.27	N/A	6.1 ± 0.58	12.3 ± 1.16	18.9 ± 3.14	N/A	28.3 ± 3.52
CI_{50}	0.610	N/A	N/A	0.956	1.400	N/A	N/A

repeated once every week for three weeks. The body weights of mice and tumor sizes were also measured by caliper measurement every 3 d. The measurements were taken in two perpendicular dimensions and tumor volumes (TV) were calculated as follows: TV (mm^3) = (The longest diameter) × (The diameter perpendicular to the longest diameter)^2/2.

The anti-tumor efficacy of each formulation was evaluated by tumor inhibition rate (TIR), which was calculated using the following formula: TIR (%) = (Control group − drug treated groups)/Control group × 100.

2.10. Statistical analysis

Measurements were carried out in triplicate. Quantitative data were presented as means ± standard deviation (SD). The analysis of variance is completed using one-way ANOVA. $P < 0.05$ was considered statistically significant.

3. Results

3.1. Characterization of LPNs and PNPs

The size, PDI, zeta potential, EE, and DL of LPNs and PNPs were determined and shown in Table 1. The sizes of D/C/LPNs and

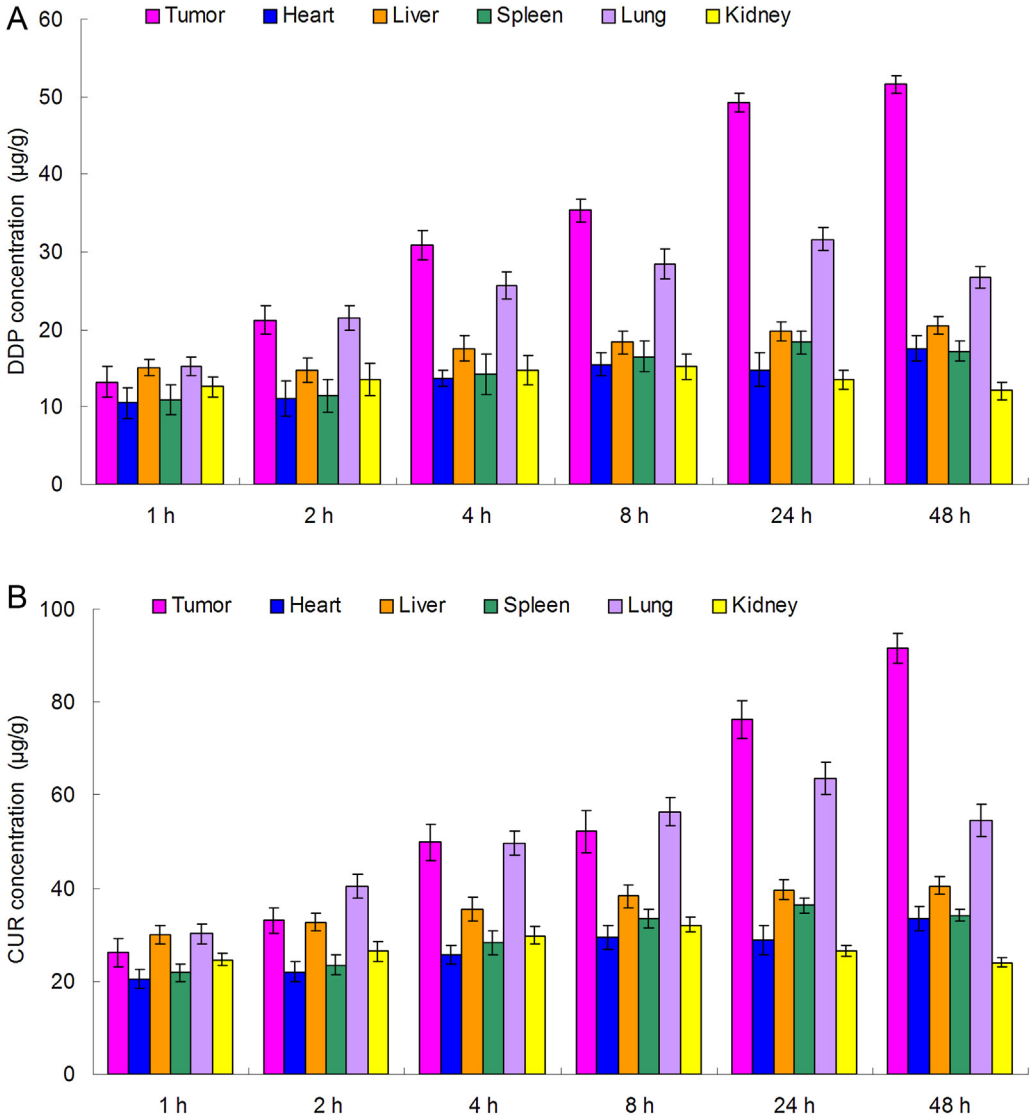

Fig. 4. *In vivo* DDP and CUR tissue distribution results of D/C/LPNs (drug concentrations are calculated as μg of drugs per g of tissue weight).

D/C/PNPs were 163.4 and 118.5 nm. The zeta potential of LPNs was lower than PNPs. The EE of DDP in D/C/LPNs and D/C/PNPs was 88.7% and 83.3%, respectively. The EE of CUR was also above 80%.

3.2. Evaluation of LPNs and PNPs stability

As depicted in Fig. 1, the average diameter of D/C/LPNs and D/C/PNPs remained stable during the first few days after formation and then gradually increased, while precipitation was barely observed. Nevertheless, the size of D/C/LPNs and D/C/PNPs increased dramatically on the 45th day after formation (after 30 days). The gradually increasing diameter of was likely caused by the degradation and aggregation of the particles. At 45 days, the aggregation of LPNs and PNPs most likely began to occur, resulting in a radical increase of size.

3.3. Release of drugs from LPNs and PNPs

The encapsulated DDP and CUR were released from the LPNs and PNPs at a sustained rate, which took over 48 h to get the complete release (Fig. 2). In the contrast, D/C solution showed rapid release and perform complete release within 4 h. The DDP and CUR released from LPNs slower than that from PNPs.

3.4. In vitro *cytotoxicity assays and synergistic effect evaluation*

MTT assay was used to investigate the *in vitro* cytotoxicity of LPNs and PNPs on HeLa cells (Fig. 3A) and HUVEC (Fig. 3B). The DDP and CUR IC_{50} values of LPNs, PNPs, and drug solutions on HeLa cells were summarized in Table 2. The DDP IC_{50} values of the D/C/LPNs were about 3 times lower than that of the D/LPNs, 5 times lower than that of the D/C/PNPs, and 9 times lower than that of the DDP solution. The CUR IC_{50} values of the D/C/LPNs were 3.8 times lower than that of the C/LPNs, 7.7 times lower than that of the D/C/PNPs, and 17.7 times lower than that of the CUR solution. The IC_{50} value of D/C/LPNs was the lowest. CI_{50} of D/C/LPNs, D/C/PNPs, and D/C solution was 0.61, 0.96 and 1.40, respectively. D/C/LPNs showed the most significant synergism effect.

3.5. In vivo *organ distribution*

In vivo DDP and CUR tissue distribution results of D/C/LPNs, D/C/PNPs, and D/C solution were shown in Fig. 4–6 respectively.

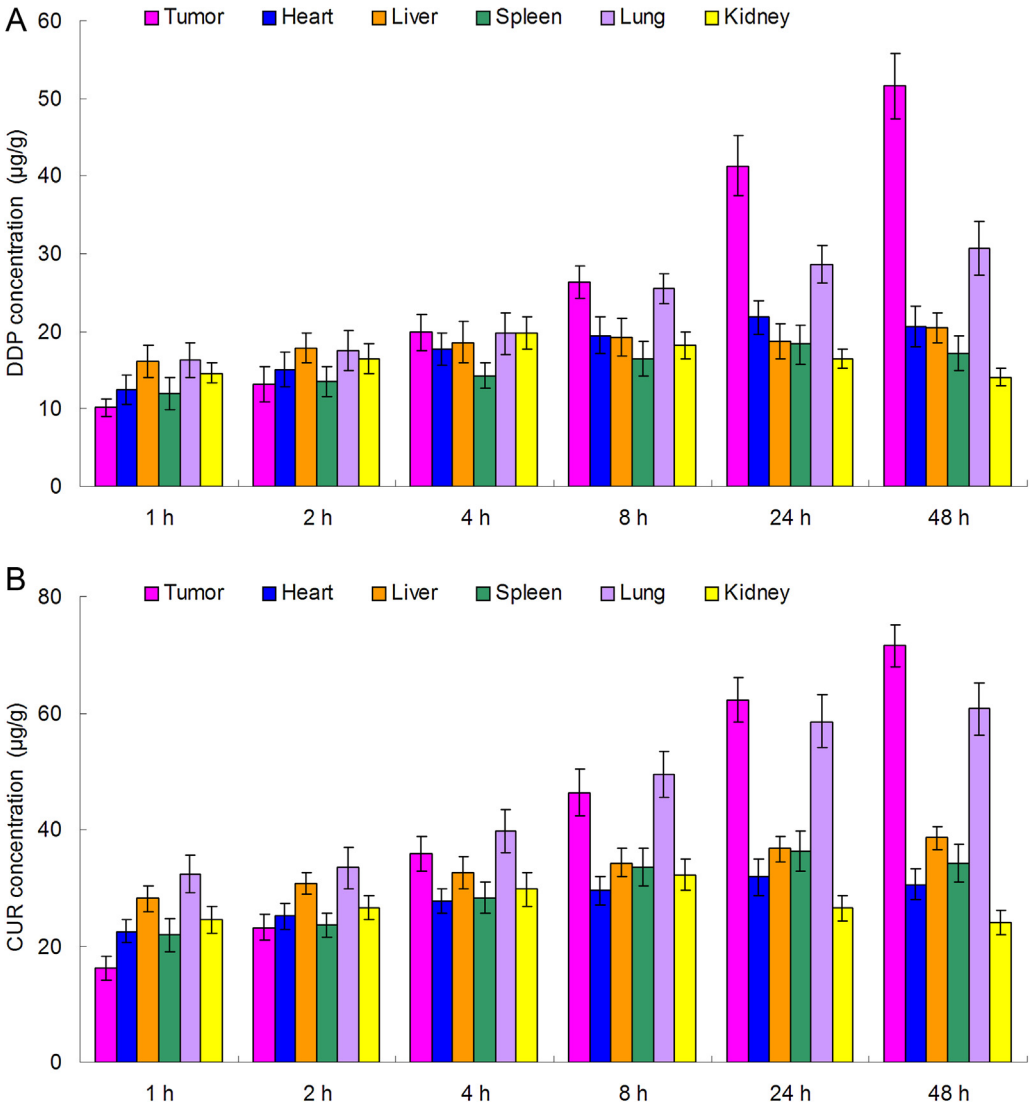

Fig. 5. *In vivo* DDP and CUR tissue distribution results of D/C/PNPs (drug concentrations are calculated as μg of drugs per g of tissue weight).

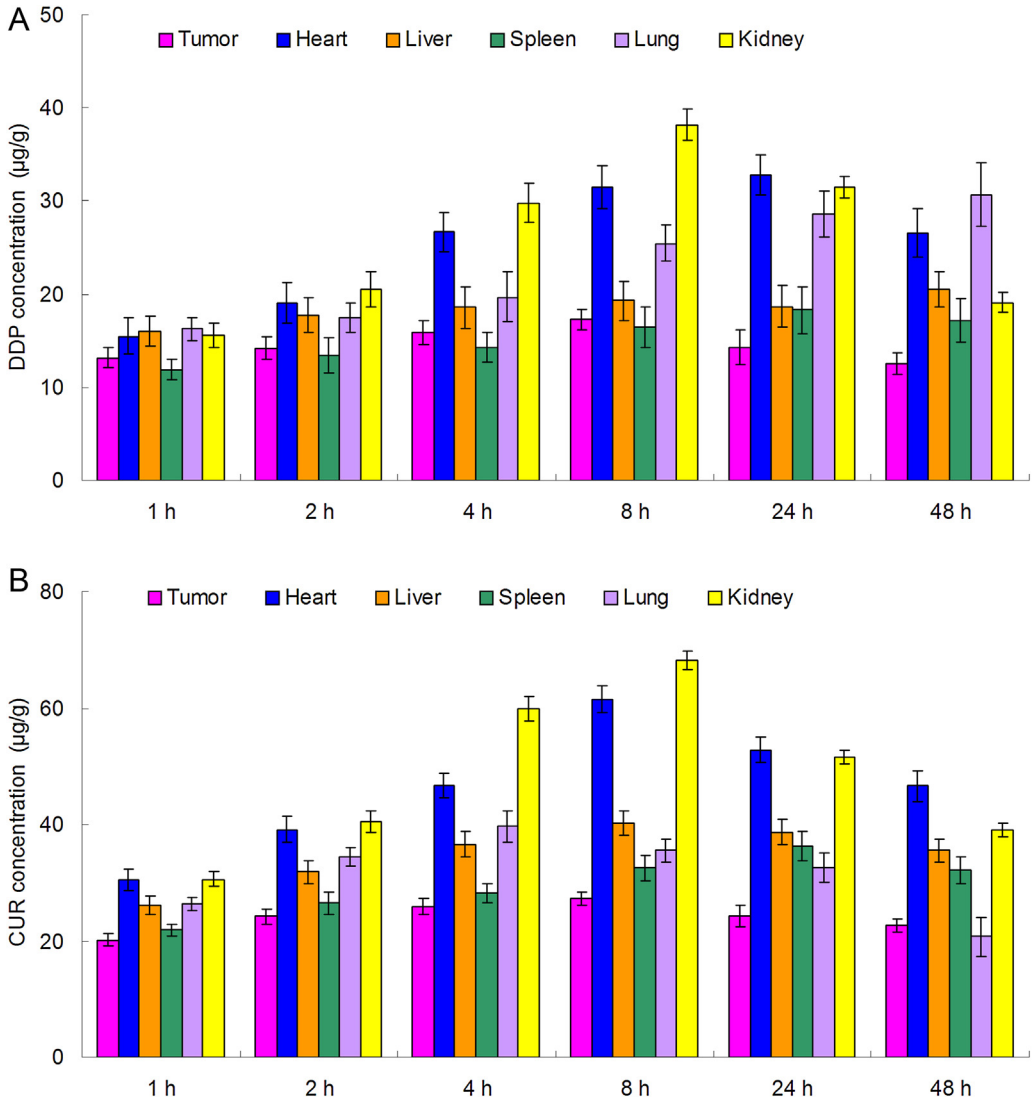

Fig. 6. *In vivo* DDP and CUR tissue distribution results of D/C solution (drug concentrations are calculated as μg of drugs per g of tissue weight).

The DDP and CUR concentration in tumor, lung and liver following injection of D/C/LPNs and D/C/PNPs was higher than the injection of D/C solution, in the meanwhile, the drug concentration of D/C/LPNs and D/C/PNPs groups in heart and kidney was lower than D/C solution. The drug concentrations of D/C/LPNs and D/C/PNPs groups in the tumor tissue remained relatively stable at all time points until 24 h and 48 h after injection, while the drug concentrations of D/C solution group reduced a lot.

3.6. In vivo *anti-tumor assays of LPNs*

The *in vivo* antitumor efficacy of LPNs was investigated on cervical cancer bearing BALB/c mice model (Fig. 7). The tumors treated with D/C/LPNs were significantly smaller than those treated with D/C/PNPs, single drug loaded LPNs, and drug solutions ($P < 0.05$). For contrast, the tumors treated with blank LPNs were similar to those treated with saline. The TIR of each group were shown in Table 3. The results suggested that the best anti-tumor effect of D/C/LPNs on cervical cancer animal.

4. Discussion

Nanoprecipitation technology was employed to prepare LPNs and PNPs [32]. The advantages of this method include its simplicity and lower energy consumption. Furthermore, it usually leads to narrow distribution and ready dispersibility of the resultant particles [33]. This method especially facilitates the incorporation of lipophilic drug into nanoparticles, thus increase the EE of the delivery systems. The sizes of D/C/LPNs (163.4 nm) were larger than that of D/C/PNPs (118.5 nm). This could be explained by the lipid shell of the LPNs, which makes the size of the particles larger than PNPs. The surface charges of D/C/LPNs and D/C/PNPs were negative. The zeta potential of LPNs was lower than PNPs. These are because the negatively charged PLGA and PEG chains. The negative surface charge of nanocarriers can reduce the systematic toxicity and were important for efficient cancer therapy [34]. The EE of DDP and CUR in D/C/LPNs and D/C/PNPs was above 80%. The results illustrated that the EE and DL of nanoparticles were not affected by the encapsulation of the two drugs, no significant difference was found with the single drug loaded carriers. For the evaluation of LPNs and PNPs stability, the average diameter of D/C/LPNs and

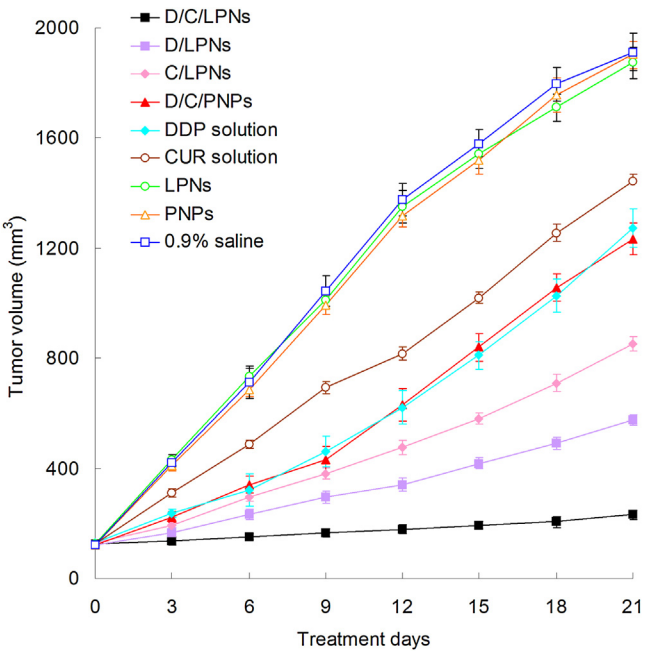

Fig. 7. The *in vivo* antitumor efficacy of LPNs and PNPs.

D/C/PNPs remained stable within the first 30 days provides support for translating these findings into future medical applications [35].

LPNs combing the mechanical advantages of biodegradable polymers and liposomes are core-shell nanoparticles structures comprising polymer cores and lipid shells [22]. These results indicate that the lipid layer at the interface of the PLGA core and the PEG shell acts as a molecular fence that helps to retain the drugs inside the NPs. The polymer cores of LPNs can entrap the DDP and CUR more tightly, thus let the drugs release slower than that of PNPs. This behavior could protect the drugs from been degraded in the circulation system. And bring about persistent therapeutic effect in the tumor site [36].

In vitro cytotoxicity assays and synergistic effect were evaluated on HeLa cells and HUVEC (Fig. 3). The IC_{50} value of D/C/LPNs was the lowest, showing the best ability in reducing viability of cervical cancer cells, exhibiting the highest *in vitro* antitumor activity. According to the Chou and Talalay's method, CI was measured to distinguish synergistic, additive, or antagonistic cytotoxic effects. $CI > 1$ represents antagonism, $CI = 1$ represents additive and $CI < 1$ represents synergism. CI_{50} of D/C/LPNs, D/C/PNPs, and D/C solution was 0.61, 0.96 and 1.40, respectively. D/C/LPNs showed the most significant synergism effect. The results illustrated that the efficiency of LPNs preformed on HeLa cells was more efficient than the PNPs ($P < 0.05$). Also, the double drugs co-delivery LPNs has better ability and showed obvious synergism effect than the single drug loaded systems. The novel carrier might have the enhanced ability to adhere to the cell membrane due to the similar nature of the lipids and the cell membrane. This character may enhance the intracellular drug accumulation and perform better in the cancer therapy [37].

Table 3
TIR of LPNs and PNPs.

Formulations	D/C/ LPNs	D/ LPNs	C/ LPNs	D/C/ PNPs	DDP solution	CUR solution
TIR (%)	87.9	69.9	55.4	35.5	33.4	24.6

In vivo DDP and CUR tissue distribution results of D/C/LPNs, D/C/PNPs, and D/C solution were shown in Figs. 4–6. The administration of drugs loaded LPNs and PNPs led to a dramatic increase of drug accumulation in the tumor tissue, as compared with the free drugs solutions. This may be explained by the theory that solid tumors have leakage micro vasculatures and the nano-sized particles could passive targeted to the tumor owing to the enhanced permeability and retention (EPR) effects [38]. EPR effects prevented the entry of the system in the normal cell at the same time favored selective entry in tumor, which resulted in the efficient drug accumulation in tumor tissue. Drug distribution in heart and kidney may cause systemic toxicity, distribution mainly less in heart and kidney could decrease the side effects and lead to better anti-tumor therapeutic efficiency.

The *in vivo* antitumor efficacy results investigated on cervical cancer bearing BALB/c mice model demonstrated that D/C/LPNs showed the strongest antitumor effect. The mechanisms may be explained as follows: 1) Utilizing the enhanced permeability and retention (EPR) effect of the cancer vasculature of solid tumors, the nanocarriers can selective delivery of drugs to the cancer site. Once delivered to the tumor, these nanocarrier-based drugs will remain in the tumor tissues for long periods of time [39]. 2) The structure of LPNs delayed drug release more than other vectors, prolonged the drug circulation time and finally increased the drug accumulation in tumor tissues [40]. 3) The lipid shell of LPNs has high affinity to the lipid cell surface, promote the fusion of the carriers to the cells, and thus deliver the drug into the tumor cells [41]. 4) The co-delivery of two drugs could get the best anti-tumor effect due to the synergetic effect of the two drugs.

5. Conclusions

In summary, newly prepared LPNs system is an effective carrier for antitumor co-delivery of DDP and CUR. LPNs prolonged the release and circulation time of the drugs and increased the accumulation of both DDP and CUR in cervical cancer cells. D/C/LPNs showed the highest cytotoxicity *in vitro* and the best antitumor efficacy *in vivo*. The effect of LPNs system might be used as an effective cervical cancer therapy strategy.

Declaration of interest

The authors report no conflicts of interest. The authors alone are responsible for the content and writing of this article.

Funding

This research did not receive any specific grant from funding agencies in the public, commercial, or not-for-profit sectors.

References

[1] N. Krieger, M.T. Bassett, S.L. Gomez, Breast and cervical cancer in 187 countries between 1980 and 2010, Lancet 379 (2012) 1391–1392.
[2] International Agency for Research on Cancer. Cervical cancer estimated incidence, mortality and prevalence worldwide in 2012. World Health Organization 2012.
[3] R. Siegel, J. Ma, Z. Zou, A. Jemal, Cancer statistics, 2014, CA. Cancer J. Clin. 64 (2014) 9–29.
[4] C. Shang, W. Zhu, T. Liu, W. Wang, G. Huang, J. Huang, P. Zhao, Y. Zhao, S. Yao, Characterization of long non-coding RNA expression profiles in lymph node metastasis of early-stage cervical cancer, Oncol. Rep. 35 (2016) 3185–3197.
[5] H. Hirte, E.B. Kennedy, L. Elit, M. Fung Kee Fung, Systemic therapy for recurrent, persistent, or metastatic cervical cancer: a clinical practice guideline, Curr. Oncol. 22 (2015) 211–219.
[6] K. Scatchard, J.L. Forrest, M. Flubacher, P. Cornes, C. Williams, Chemotherapy for metastatic and recurrent cervical cancer, Cochrane Database Syst. Rev. 10 (2012) CD006469.

[7] Z. Wang, J. Lv, T. Zhang, Combination of IL-24 and cisplatin inhibits angiogenesis and lymphangiogenesis of cervical cancer xenografts in a nude mouse model by inhibiting VEGF, VEGF-C and PDGF-B, Oncol. Rep. 33 (2015) 2468–2476.
[8] I. Cadron, T. Van Gorp, F. Amant, K. Leunen, P. Neven, I. Vergote, Chemotherapy for recurrent cervical cancer, Gynecol. Oncol. 107 (2007) S113–8.
[9] A. Macciò, Madeddu C. Cisplatin, an old drug with a newfound efficacy – from mechanisms of action to cytotoxicity, Expert Opin. Pharmacother. 14 (2013) 1839–1857.
[10] S. Ugur, R. Ulu, A. Dogukan, A. Gurel, I.P. Yigit, N. Gozel, B. Aygen, N. Ilhan, The renoprotective effect of curcumin in cisplatin-induced nephrotoxicity, Ren. Fail. 37 (2015) 332–336.
[11] H. Kulhari, D. Pooja, M.K. Singh, A.S. Chauhan, Optimization of carboxylate-terminated poly(amidoamine) dendrimer-mediated cisplatin formulation, Drug Dev. Ind. Pharm. 41 (2015) 232–238.
[12] P. Chen, J. Li, H.G. Jiang, T. Lan, Y.C. Chen, Curcumin reverses cisplatin resistance in cisplatin-resistant lung caner cells by inhibiting FA/BRCA pathway, Tumour Biol. 36 (2015) 3591–3599.
[13] Y. Wang, P.C. Hu, F.F. Gao, J.W. Lv, S. Xu, C.C. Kuang, L. Wei, J.W. Zhang, The protective effect of curcumin on hepatotoxicity and ultrastructural damage induced by cisplatin, Ultrastruct. Pathol. 38 (2014) 358–362.
[14] M. Singh, N. Singh, Molecular mechanism of curcumin induced cytotoxicity in human cervical carcinoma cells, Mol. Cell. Biochem. 325 (2009) 107–119.
[15] M.S. Zaman, N. Chauhan, M.M. Yallapu, R.K. Gara, D.M. Maher, S. Kumari, M. Sikander, S. Khan, N. Zafar, M. Jaggi, S.C. Chauhan, Curcumin nanoformulation for cervical cancer treatment, Sci. Rep. 6 (2016) 20051.
[16] W. Sajomsang, P. Gonil, S. Saesoo, U.R. Ruktanonchai, W. Srinuanchai, S. Puttipipatkhachorn, Synthesis and anticervical cancer activity of novel pH responsive micelles for oral curcumin delivery, Int. J. Pharm. 477 (2014) 261–272.
[17] M. Zheng, S. Liu, X. Guan, Z. Xie, One-step synthesis of nanoscale zeolitic imidazolate frameworks with high curcumin loading for treatment of cervical cancer, ACS Appl. Mater. Interfaces 7 (2015) 22181–22187.
[18] M.J. Tuorkey, Curcumin a potent cancer preventive agent: mechanisms of cancer cell killing, Interv. Med. Appl. Sci. 6 (2014) 139–146.
[19] M. Roy, S. Mukherjee, Reversal of resistance towards cisplatin by curcumin in cervical cancer cells, Asian Pac. J. Cancer Prev. 15 (2014) 1403–1410.
[20] H.S. Oberoi, N.V. Nukolova, A.V. Kabanov, T.K. Bronich, Nanocarriers for delivery of platinum anticancer drugs, Adv. Drug Deliv. Rev. 65 (2013) 1667–1685.
[21] J. Panyam, V. Labhasetwar, Biodegradable nanoparticles for drug and gene delivery to cells and tissue, Adv. Drug Deliv. Rev. 55 (2003) 329–347.
[22] K. Hadinoto, A. Sundaresan, W.S. Cheow, Lipid-polymer hybrid nanoparticles as a new generation therapeutic delivery platform: a review, Eur. J. Pharm. Biopharm. 85 (2013) 427–443.
[23] B. Mandal, H. Bhattacharjee, N. Mittal, H. Sah, P. Balabathula, L.A. Thoma, G.C. Wood, Core-shell-type lipid-polymer hybrid nanoparticles as a drug delivery platform, Nanomedicine 9 (2013) 474–491.
[24] J. Singh, G. Chhabra, K. Pathak, Development of acetazolamide-loaded, pH-triggered polymeric nanoparticulate in situ gel for sustained ocular delivery: in vitro: ex vivo evaluation and pharmacodynamic study, Drug Dev. Ind. Pharm. 40 (2014) 1223–1232.
[25] W. Zou, G. Cao, Y. Xi, N. Zhang, New approach for local delivery of rapamycin by bioadhesive PLGA-carbopol nanoparticles, Drug Deliv. 16 (2009) 15–23.
[26] W. Zou, C. Liu, Z. Chen, N. Zhang, Studies on bioadhesive PLGA nanoparticles: a promising gene delivery system for efficient gene therapy to lung cancer, Int. J. Pharm. 370 (2009) 187–195.
[27] L. Rao, Y. Ma, M. Zhuang, T. Luo, Y. Wang, A. Hong, Chitosan-decorated selenium nanoparticles as protein carriers to improve the in vivo half-life of the peptide therapeutic BAY 55–9837 for type 2 diabetes mellitus, Int. J. Nanomed. 9 (2014) 4819–4828.
[28] B. Wang, H. Li, Q. Yao, Y. Zhang, X. Zhu, T. Xia, J. Wang, G. Li, X. Li, S. Ni, Local in vitro delivery of rapamycin from electrospun PEO/PDLLA nanofibers for glioblastoma treatment, Biomed. Pharmacother. 83 (2016) 1345–1352.
[29] X.B. Wang, H.Y. Zhou, Molecularly targeted gemcitabine-loaded nanoparticulate system towards the treatment of EGFR overexpressing lung cancer, Biomed. Pharmacother. 70 (2015) 123–128.
[30] S. Lv, Z. Tang, M. Li, J. Lin, W. Song, H. Liu, Y. Huang, Y. Zhang, X. Chen, Co-delivery of doxorubicin and paclitaxel by PEG-polypeptide nanovehicle for the treatment of non-small cell lung cancer, Biomaterials 35 (2014) 6118–6129.
[31] P.X. Li, J.H. Mu, H.L. Xiao, D.H. Li, Antitumor effect of photodynamic therapy with a novel targeted photosensitizer on cervical carcinoma, Oncol. Rep. 33 (2015) 125–132.
[32] S. Martín-Saldaña, R. Palao-Suay, A. Trinidad, M.R. Aguilar, R. Ramírez-Camacho, J. San Román, Otoprotective properties of 6α-methylprednisolone-loaded nanoparticles against cisplatin: in vitro and in vivo correlation, Nanomedicine 12 (2016) 965–976.
[33] J. Du, X. Li, H. Zhao, Y. Zhou, L. Wang, S. Tian, Y. Wang, Nanosuspensions of poorly water-soluble drugs prepared by bottom-up technologies, Int. J. Pharm. 495 (2015) 738–749.
[34] D. Mandal, S. Kumar Dash, B. Das, S. Chattopadhyay, T. Ghosh, D. Das, S. Roy, Bio-fabricated silver nanoparticles preferentially targets Gram positive depending on cell surface charge, Biomed. Pharmacother. 83 (2016) 548–558.
[35] G.J. Charrois, T.M. Allen, Drug release rate influences the pharmacokinetics, biodistribution, therapeutic activity, and toxicity of pegylated liposomal doxorubicin formulations in murine breast cancer, Biochim. Biophys. Acta 1663 (2004) 167–177.
[36] K. Hadinoto, A. Sundaresan, W.S. Cheow, Lipid-polymer hybrid nanoparticles as a new generation therapeutic delivery platform: a review, Eur. J. Pharm. Biopharm. 85 (2013) 427–443.
[37] C.W. Su, M.Y. Chiang, Y.L. Lin, N.M. Tsai, Y.P. Chen, W.M. Li, C.H. Hsu, S.Y. Chen, Sodium dodecyl sulfate-Modified doxorubicin-loaded chitosan-lipid nanocarrier with multi polysaccharide-lecithin nanoarchitecture for augmented bioavailability and stability of oral administration in vitro and In vivo, J. Biomed. Nanotechnol. 12 (2016) 962–972.
[38] J. Choi, E. Ko, H.K. Chung, J.H. Lee, E.J. Ju, H.K. Lim, I. Park, K.S. Kim, J.H. Lee, W.C. Son, J.S. Lee, J. Jung, S.Y. Jeong, S.Y. Song, E.K. Choi, Nanoparticulated docetaxel exerts enhanced anticancer efficacy and overcomes existing limitations of traditional drugs, Int. J. Nanomed. 10 (2015) 6121–6132.
[39] J. Park, N.R. Kadasala, S.A. Abouelmagd, M.A. Castanares, D.S. Collins, A. Wei, Y. Yeo, Polymer-iron oxide composite nanoparticles for EPR-independent drug delivery, Biomaterials 101 (2016) 285–295.
[40] X. Zhao, F. Li, Y. Li, H. Wang, H. Ren, J. Chen, G. Nie, J. Hao, Co-delivery of HIF1α siRNA and gemcitabine via biocompatible lipid-polymer hybrid nanoparticles for effective treatment of pancreatic cancer, Biomaterials 46 (2015) 13–25.
[41] S. Colombo, D. Cun, K. Remaut, M. Bunker, J. Zhang, B. Martin-Bertelsen, A. Yaghmur, K. Braeckmans, H.M. Nielsen, C. Foged, Mechanistic profiling of the siRNA delivery dynamics of lipid-polymer hybrid nanoparticles, J. Control. Release 201 (2015) 22–31.